International Journal of Fuzzy Logic and Intelligent Systems, vol. 8, no. 1, March 2008 pp. 24-30

# Dynamic Simulation of AGC/LPC Synthetical System for Hot Strip Finishing Mill

**Xiaoying Wang and Jingcheng Wang***

**Department of Automation, Shanghai Jiao Tong University**
**Shanghai, 200240, China**

## Abstract

A simulation of hot strip finishing mill automatic gauge control (AGC) system is built, which is divided into four modules such as rolling mill system, AGC module, looper system and strip model. The rolling mill system is built by mechanism modeling, the looper system and strip model are built by function modeling, and the AGC model is tried to use intelligent control of a multi-function AGC system. The target is attempted to use this simulation object to minimize finisher exit strip thickness deviation resulting from strip entry thickness disturbance and rolling force deviation. Simulation results show that the result of this AGC/LPC synthetical system module simulation is quite close to the actual result. The simulation system can also analyze most kinds of disturbance which affect the rolling process. It is proved that the system can represent practical situation of hot strip finishing mill process control, and be used as a basic platform of research and development for researcher and engineer.

**Key Words** : Automatic gauge control (AGC), Looper process control (LPC), Tension control system, Deviation

## 1. Introduction

Equipments layout of locale finishing mill is shown in Fig. 1. Hot rolling process should be treated as a whole because of coupling phenomenon between the strip thickness, which is controlled by AGC system, and strip mass flow and tension which are controlled by looper system. Furthermore, there exist interactions among stands. In conventional control, these interactions are omitted. With the mill press-down system changes from electric style to hydraulic style and higher demands of the customers, the interactions between AGC system and looper system can't be neglected and are becoming the key point of further enhancement of product quality. Synthetical control research of AGC/LPC system is urgent [1]-[3].

From paper [4]-[6], in order to joint the AGC and LPC subsystem, the main drive control system must be added. The rolling speed which is got from the drive system is considered as the interface of the AGC/LPC. In this paper, the forward slip and backward slip deviation are considered. In the conventional module, the drive control system is added to the AGC and looper control system, and then the module becomes more complex and unstable. According to the definition of the forward slip and backward slip, after the deviation of the forward slip and backward slip is got, the strip entry speed and exit speed will be clear. This paper adopted more exact rolling force forecasting model and each simulation module is corresponding to locale, so it is more convenient for adjusting parameters as locale.

The rest of this paper is organized as follows. The model of synthetical system for hot strip finishing mill system is built in section 2. Section 3 shows the simulation result followed by the conclusions in section 4.

## 2. Modeling of the system

According to the locale, the simulation system considered for the corresponding objects can be organized as given in Fig. 2, which is divided into several parts as rolling mill system, LPC system, AGC module and strip.

### 2.1 Rolling mill system

In this paper, finishing mill system consists of rolling force module, hydraulic pressure module, stand model and drive module.

#### 2.1.1 Rolling force module

Based on P.M.Cook and A.W.MC Crum model [7], and considering much for steady state, the system can be modeled as equation (1), which has been tested by several strips almost entirely close to actual force.

Manuscript received Jan. 24, 2008; revised Mar. 10, 2008.
*Corresponding Author: jcwang@sjtu.edu.cn
This work was supported by National 863 Plan of China (No.2006AA040308, No.2007AA041403) and Shanghai Rising-Star Program (No.07QA14030).

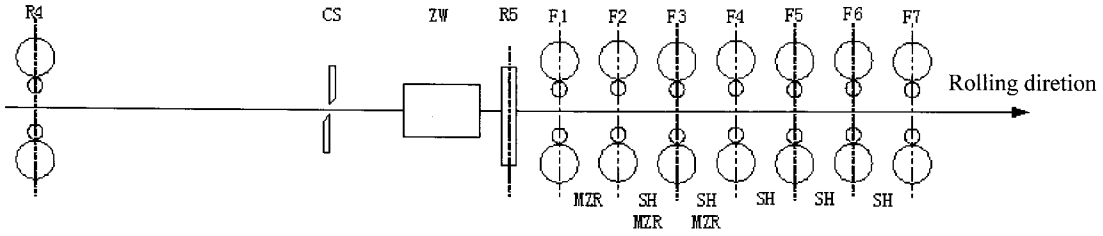


R4 is roughing mill; CS is flying shear; ZW is phosphorus removal box; R5 is guide roller; F1 to F7 are finishing mills; MZR is minimal tension control system; SH is looper.

Fig. 1. Equipments layout of finishing mill

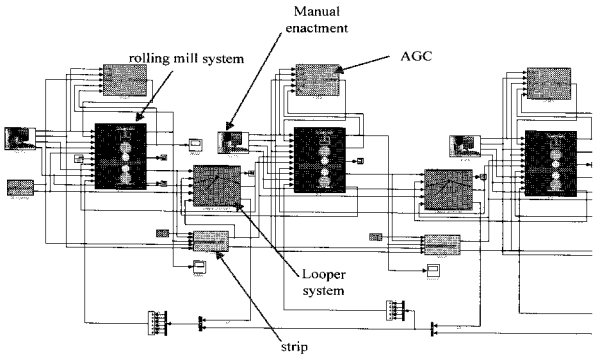


Fig. 2. Dynamic simulation of the synthetical system

$$F = W \cdot l_d \cdot K_m \cdot Q_F \cdot N_t \tag{1}$$

where $F$ is rolling force, $W$ is strip width, $l_d$ is staving contact arc length, $K_m$ is material distortion resisting force, $Q_F$ is outside friction effect coefficient and $N_t$ is tension coefficient.

(1) Staving contact arc length $l_d$ is calculated by staving roller radius and depressive quantity $\Delta h$.

$$l_d = \sqrt{R'\Delta h} \tag{2}$$

$$R' = R \cdot \left(\frac{B + \sqrt{B^2 + 4 \cdot A \cdot \Delta h}}{2 \cdot A}\right)^2 \tag{3}$$

where $\Delta h = H - h$ is press quantity and $R$ is roller radius. $A$ and $B$ are calculated as follows.

$$A = \Delta h - \frac{16 \cdot \left((1-\upsilon^2)\right)}{\pi \cdot E} \cdot k_m \cdot q_2(r) \cdot R \cdot \sqrt{\frac{r}{1-r}} \tag{4}$$

$$B = \frac{16 \cdot \left(1-\upsilon^2\right)}{\pi \cdot E} \cdot k_m \cdot q_1(r) \cdot \sqrt{R \cdot \Delta h} \tag{5}$$

where $\upsilon$ is roller's Poisson ratio, $E$ is Young Modulus.

$$\begin{aligned} q_1(r) &= a_{F1} + a_{F2} \cdot r \\ q_2(r) &= a_{F3} + a_{F4} \cdot r + a_{F5} \cdot r^2 \end{aligned} \tag{6}$$

where $r$ is depressive rate, $a_{F1}$ to $a_{F5}$ are rolling force model parameters.

(2) Outside friction effect coefficient $Q_F$

$$Q_F = q_1(r) + q_2(r) \cdot \sqrt{\frac{R'}{h}} \tag{7}$$

where $h$ is exit strip thickness.

(3) Material distortion resisting force $K_m$

$$\begin{aligned} K_m = &\left\{a_{k0} + \sum_{i=1}^{9}\left(a_{ki}\rho_i\right)\right\} * \\ &\exp\left[b_{k0} + b_{k1}\rho_c + b_{k2}\frac{1}{T_k}\right] \varepsilon^{b_{k3}} u^{b_{k4}} \end{aligned} \tag{8}$$

where $\rho_i$ denotes chemistry component content such as C, Si, Mn, Ni, Cr, Ti, Mo, V, Nb. $\rho_c$ is C component content, $T_k$ is material thermodynamics temperature, $\varepsilon = \ln(\frac{H}{h})$ is material distortion degree in the rolling process, $u = (\varepsilon * v)/\sqrt{R*(H-h)}$ is material distortion velocity, where $v$ is roller velocity, $a_{ki}$ is each component coefficient, $b_{ki}$ is each basic term coefficient.

(4) Tension coefficient $N_t$

$$N_t = 1 - [\xi \cdot Ten\_b + (1-\xi) \cdot Ten\_f] / K_m \tag{9}$$

where $\xi$ is back tension weighting coefficient, $Ten\_b$ is back tension, $Ten\_f$ is front tension.

Hence, all the rolling force effect factors such as relative reduction rate, exiting strip thickness, exiting strip width, aimed strip gauge, entering strip velocity, strip tension and contents of C, Si, Mn, P, S, Cu have been considered. It is obviously that above rolling force model is more comprehensive and accurate than P.M.Cook and A.W.MC Crum model.

### 2.1.2 Hydraulic pressure module

Hydraulic pressure module is mainly composed of servo valve and hydraulic cylinder.

(1) Servo valve

When hydraulic implement machine's natural frequency is less than 50 Hz, the relationship between valve core displacement and input control electric current can be estimated

as

$$\frac{x(s)}{I(s)} = \frac{K_v}{s/\varpi_v + 1} \tag{10}$$

where $x(s)$ is valve core displacement, $I(s)$ is control electric current, $\omega_v$ is servo valve natural frequency, $K_v$ is servo valve magnify coefficient, $s$ is Laplace Operator.

When servo valve positive onset and oil headstream connect with laden cavity, the flux equation is given as follows.

$$Q_v = C_d \cdot \omega \cdot x(s)\sqrt{\frac{2}{\rho}(P_s - P_c)} \quad (P_s > P_c) \tag{11}$$

$$\mathrm{Q_v} = -\mathrm{C_d} \cdot \omega \cdot \mathrm{x(s)}\sqrt{\frac{2}{\rho}(\mathrm{P_c} - \mathrm{P_s})} \quad (P_c > P_s) \tag{12}$$

When servo valve negative onset and oil headstream connect with laden cavity, the flux equation is given as follows.

$$\mathrm{Q_v} = \mathrm{C_d} \cdot \omega \cdot \mathrm{x(s)}\sqrt{\frac{2}{\rho}\mathrm{P_c}} \quad (P_c > 0) \tag{13}$$

$$\mathrm{Q_v} = -\mathrm{C_d} \cdot \omega \cdot \mathrm{x(s)}\sqrt{-\frac{2}{\rho}\mathrm{P_c}} \quad (P_c < 0) \tag{14}$$

where $P_s$ is oil headstream pressure, $P_c$ is laden pressure, $C_d$ is servo valve flux coefficient, $\omega$ is servo valve area grads, $\rho$ is oil density.

(2) Hydraulic cylinder

According to hydraulic cylinder flux balance formula, front cavity pressure of hydraulic cylinder is calculated as follows.

$$\frac{\mathrm{dP_c}}{\mathrm{dt}} = \frac{\beta_e}{\mathrm{V_c} + \mathrm{A_c x_p}}(\mathrm{Q_v} - \mathrm{A_c}\frac{\mathrm{dx_p}}{\mathrm{dt}} - \mathrm{C_l}(\mathrm{P_c} - \mathrm{P_h})) \tag{15}$$

where $\beta_e$ is hydraulic oil elastic modulus, $V_c$ denotes bulk of hydraulic cylinder front cavity, $x_p$ is hydraulic cylinder output displacement, $C_l$ is hydraulic cylinder leak coefficient, $P_h$ is pressure of hydraulic cylinder back cavity, $P_c$ is pressure of hydraulic cylinder front cavity, $A_c$ is virtual area of hydraulic cylinder front cavity. Additionally, back cavity of hydraulic cylinder is kept on constant pressure according to locale.

### 2.1.3 Stand model

Based on the lumped principle, the single stand can be predigested as spring-dumping system and each part is quality system alone. There are two cases for hydraulic cylinder and piston. One case is that hydraulic cylinder fixed on mill housing and piston fixed on bearing pedestal. In this case, hydraulic cylinder is comparatively immobility and piston is up and down when rolling. Another case is on the reverse. In this paper, upper column, crossbeam and piston of hydraulic cylinder are considered as the first quality system, while bearing pedestal and hydraulic cylinder block are considered as the second quality system. Upper backup and work roller are considered as the third quality system, then down work and backup roller with bearing pedestal and down mill housing are considered as the fourth quality system. Hence, the actual load stand can be predigested as a four degree-of-freedom spring-dumping system as in Fig. 3. In this paper, rollers' weight is balanced by hydraulic pressure and friction is almost linear.

According to mechanics balance principle, roll system loading equation can be expressed as follows.

$$\begin{aligned}
\Delta P &= m_0\ddot{x}_0 + c_0(\dot{x}_0 - \dot{x}_1) + k_0 x_0 \\
-\Delta P &= m_1\ddot{x}_1 + c_0(\dot{x}_1 - \dot{x}_0) + c_1(\dot{x}_1 - \dot{x}_2) + k_1(x_1 - x_2) \\
F_W &= m_2\ddot{x}_2 + c_1(\dot{x}_2 - \dot{x}_1) + k_1(x_2 - x_1) \\
-F_W &= m_3\ddot{x}_3 + c_2\dot{x}_3 + k_2 x_3
\end{aligned} \tag{16}$$

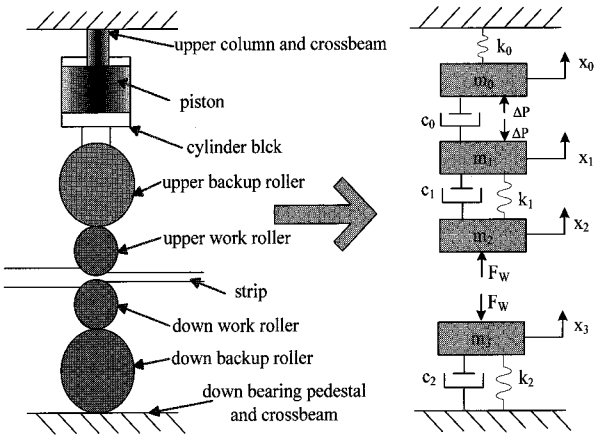


Fig. 3. stand predigested as spring-dumping system

where $m_0$, $m_1$, $m_2$ and $m_3$ are the equivalent total weight of first, second, third and fourth quality system respectively. $x_0$, $x_1$, $x_2$ and $x_3$ are the centroid displacement of first, second, third and fourth quality system respectively, $c_0$ is the equivalent damping of piston and hydraulic cylinder block, $c_1$ is the equivalent damping of bearing pedestal and upper backup and work roller, $c_2$ is the equivalent damping of down roller system, $k_0$ is the equivalent stiffness of upper part of stand, $k_1$ is the equivalent stiffness of upper backup and work roller, $k_2$ is the equivalent stiffness of down roller system, $\Delta P$ is output pressure of hydraulic cylinder, $F_w$ is the rolling force on strip.

### 2.1.4 Drive module

This module, as give in (17) to (19), calculates the real-time linear velocity of roller, exit strip and entry strip.

$$\mathrm{V_r} = \mathrm{V_0}(\eta + 1)\frac{1}{\mathrm{Ts} + 1} \tag{17}$$

where $V_r$ is real-time linear velocity of roller, $V_0$ is the initial linear velocity of roller, $\eta$ is speed ratio which calculated in looper system, $T$ is roller's response cycle.

Then considering slip, strip velocity is approximated as follows.

$$\begin{aligned} V_{stripout} &= V_r(1+\phi) \\ V_{stripin} &= V_{stripout}\, h/H \end{aligned} \tag{18}$$

where $V_{stripout}$ is strip exit velocity, $V_{stripin}$ is strip entry velocity, $\phi$ is slip, $h$ is strip exit thickness, $H$ is strip entry thickness.

From (1) to (18), a block diagram of the finishing mill can be obtained as shown in Fig. 4.

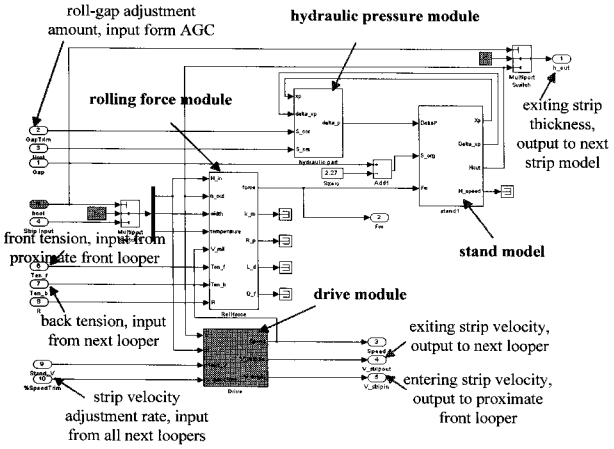


Fig. 4. Finishing mill system

## 2.2 Looper system

A looper installed at inter-stand position reduces tension variation by changing its angle, so it can also contribute to the quality of the products. Moreover, it enable stable operation of the process by absorbing an excessive loop of the strip arising from a moss flow unbalance. Therefore, the looper angle should be kept to a specified value during operation in order to maintain maximum flexibility for sudden mass flow changes. In summary, looper and tension control is achieved by simultaneous control of the strip tension and looper angle. However, this is a difficult control problem because of significant interaction and need for high performance in the presence of significant uncertainties coming from disturbances and model mismatch. Many methods [8]-[13] have proposed and applied to this control problem, they are limited to passively adjust looper angle or height to keep tension and strip velocity comparatively stable. But looper angle is changed obviously in site sometimes. In fact, strip velocity change is the main cause of tension change. Active control strip velocity is tried in this paper to control tension.

Looper system is used to adjust strip velocity when the speed of front stand exiting strip is unequal to the speed of next stand entering strip, then strip tension will change at the same time. So looper system is designed as strip tension and strip velocity adjustment percentage calculation. Tension is expressed as follows

$$T_s = \frac{A \cdot E}{L} \int_0^{t_s} (v_{i,out} - v_{i+1,in})dt \tag{19}$$

where $T_s$ is strip tension, $A$ is cross sectional area of strip, $L$ is the distance between two adjacent stands, $v_{i,out}$ is the speed of front stand exiting strip, $v_{i+1,in}$ is the speed of next stand entering strip.

With the aim to control finishing rolling temperature and make finishing mills matched with coiler better, velocity of terminal stand is used as reference can't be adjusted. So the direction of speed adjustment is from latter looper to all frontal finishing mills. Strip velocity adjustment percentage is approximated as follows.

$$\eta = \frac{100 \int_0^{t_s} (v_{i+1,in} - v_{i,out})dt}{V_0} \tag{20}$$

where $\eta$ is strip velocity adjustment percent, $v_0$ is the initial linear velocity of the adjacent front roller.

So looper system can be simulated as shown in Fig. 5.

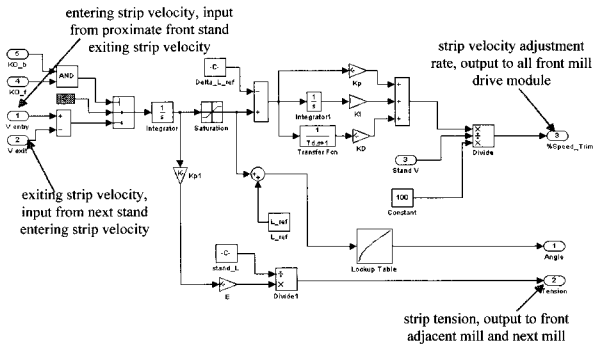


Fig. 5. Looper system

## 2.3 Strip module and manual enactment module

Strip of this simulation system is data stream in nature. Strip includes temperature, velocity, thickness, width and so on. The main function of strip is to contact finishing mills. Hence, strip is mostly considered for transfer delay among stands. Additionally, temperature drop for water cooling is estimated as follows.

$$T_{out} = (T_{in} - T_w)e^{-\gamma} + T_w \tag{21}$$

where $T_{out}$ is output strip

## 2.4 AGC module

This module is used to control gauge in real-time. Any new

method can be tried by adding new model in this part. According to theoretical research and much experience of produce debugging, multi-frame multi-function AGC comprehensive control scheme is used as given in Fig.7 in this paper.

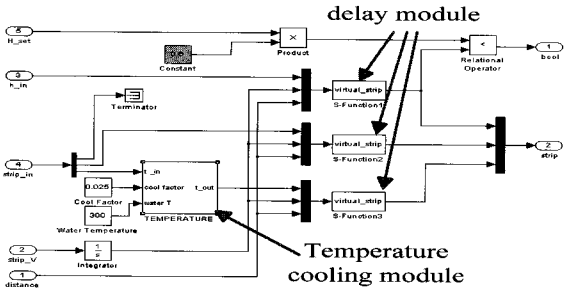


Fig. 6. Strip module

Intelligence of comprehensive function and control parameter is shown as follows:

if $(|P_1 - P_0| \le 500kN)$ then $(KO_1 = KO_2 = KO_3 = 0)$ KFFAGC of F2, F3 and F4 are working (where $P_0$ is locking pressure).

if $(500kN < |P_1 - P_0| \le 800kN)$ then $(KO_1 = 1, KO_2 = KO_3 = 0)$ KFFAGC of F2, F3 , F4 and F5 are working.

if $(800kN < |P_1 - P_0| \le 1200kN)$ then $(KO_1 = KO_2 = 1, KO_3 = 0)$ KFFAGC of F2, F3 , F4, F5 and F6 are working.

if $(|P_1 - P_0| > 1200kN)$ then $(KO_1 = KO_2 = KO_3 = 1)$ KFFAGC of F2, F3 , F4, F5 and F6 are working.

if $(h_0 \le 4.0mm)$ then $(KO_4 = 0)$ MAGC of F6 and F7 are working (where . $h_0$ is X-ray monitor measured thickness of strip).

if $(h_0 > 4.0mm)$ then $(KO_4 = 1)$ MAGC of F5, F6 and F7 are working.

$G_4 = (P_5 - 5000)/(15000 - 5000) + 0.5$

$G_5 = (P_6 - 5000)/(15000 - 5000) + 0.5$

$G_1 = 2/h_7$

$G_2 = 1.5/h_7$

$G_1 = 1.2/h_7$

(where $P_5$ and $P_6$ are roll force of F6 and F7 respectively, $h_7$ is actual thickness of F7 exiting strip).

(1) Hardness feed forward AGC (KFFAGC)

In this paper, hardness feed forward AGC is used rather than classical thickness feed forward AGC. It is because that incoming material thickness fluctuation can be easily eliminated and is not long-term hereditary in hot rolling process. On the contrary, incoming material hardness fluctuation which is caused by temperature fluctuation is greatly effect on exiting strip thickness quality and it has strong hereditary. Hence, F1 is used as a hardness measuring frame and there is no AGC executed on it. Then input mode and control rate of hardness feed forward of F2 to F7 is determined by fluctuation of slab hardness which is calculated by on-line measured rolling force. KFFAGC adjustment amount of roll gap is approximated as follows:

$$\Delta S_{kffi} = -\frac{\partial P_i}{\partial K_i} \cdot \frac{\Delta K_1}{M} = -K_{kffi} \cdot \Delta K_1 \qquad (22)$$

Where $\Delta S_{kffi}$ is KFFAGC adjustment amount of roll gap of $F_i$, $P_i$ is rolling force of $F_i$, $K_i$ is hardness of strip of $F_i$, $M$ is rolling stiffness coefficient, $K_{kffi}$ is hardness feed forward reduction effect coefficient and $\Delta K_1$ is strip hardness variable quantity of $F_i$.

(2) Pressure feedback AGC (GM-AGC)

GM-AGC is just used on F5 and F6 because its action cycle is too short and it needed to be frequently adjusted. Its adjustment amount of roll gap is approximated as follows:

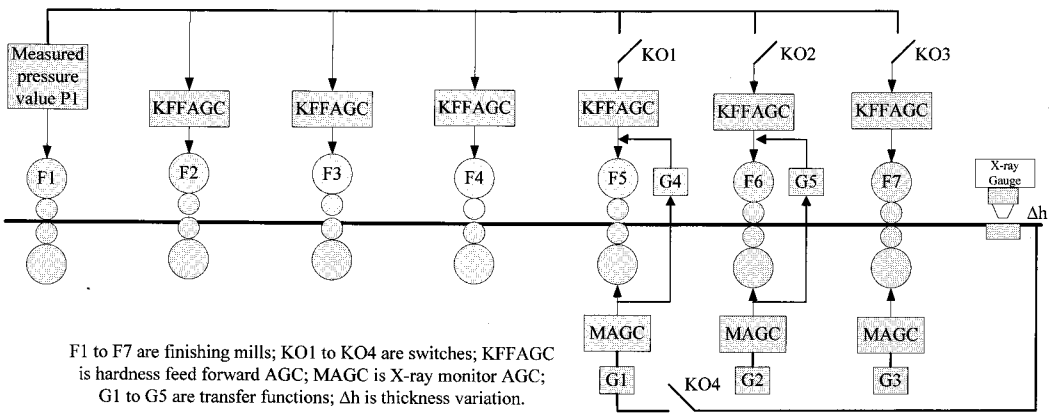


F1 to F7 are finishing mills; KO1 to KO4 are switches; KFFAGC is hardness feed forward AGC; MAGC is X-ray monitor AGC; G1 to G5 are transfer functions; Δh is thickness variation.

Fig.7. Scheme of multi-function AGC control

$$\Delta S_{gi} = -\left[(M+Q)/M(h_i - h_{0i}) - (s_i - s_{0i})\right]$$
$$h_i = s_i + \frac{P_i}{M} \quad (23)$$

where $\Delta S_{gi}$ is GM-AGC adjustment amount of roll gap of $F_i$, $h_i$ is actual thickness of $F_i$ exiting strip, $h_{0i}$ is objective thickness of $F_i$ exiting strip, $s_i$ is actual roll gap value of $F_i$, $s_{0i}$ is objective roll gap value of $F_i$, $Q$ is rolled piece plasticity coefficient and $\frac{M+Q}{M}$ is reduction compensation coefficient.

(3) Monitor AGC (MAGC)

MAGC is controlled by X-ray monitor which is installed behind F7. Its monitoring compensation quantity $\Delta S_m$ is approximated as follows:

$$\Delta S_m = \Delta S_{ms} \cdot K_{MMON}$$
$$K_{MMON} = 1 + K_{MMoni} \cdot \frac{C_M}{C_G} \quad (24)$$

where $\Delta S_{ms}$ is initial setting value of monitoring correction value, $K_{MMON}$ is MAGC coefficient, $K_{MMoni}$ is attenuation coefficient, $C_M$ is rolled piece plastic stiffness and $C_G$ is mill rigidity.

From (1) - (24), a block diagram of the synthetical system can be obtained which is shown in Fig.2. It is obvious that roller's speed and strip tension effect rolling force consequently effect exiting strip thickness in single mill, back rollers' speed effect front rollers' speed, and strip tension is effected by strip velocity and strip thickness variance. Hence, interactions and coupling phenomena among mills are clear. The manual enactment module is just used to manual control some parameters such as required exit strip thickness, roller gap position and initial linear velocity of work roller before each simulation.

## 3. Simulation

In order to get more accurate result of the synthetical control system, level 2 initial setting parameters in manual enactment model are from the field actual data as given in Table 1. Under this condition, there is no disturbance phenomenon, the strip exit thickness of the total seven stands are shown in Fig. 8. It is obviously that the synthetical system is realized biting strip, normal rolling and throwing strip.

To simplify analysis procedure, the strip entry thickness disturbance and entry force disturbance at F1 stand are considered, under these disturbance conditions, the strip exit thickness of the total seven stands are analyzed.

Table 1. Level 2 initial setting parameters

| No. stand | F1 | F2 | F3 | F4 | F5 | F6 | F7 |
|---|---|---|---|---|---|---|---|
| Exit thickness expected (mm) | 20 | 15 | 10 | 7 | 5 | 3.5 | 3 |
| Rolling force P(T) | 2822.87 | 2782.94 | 2496.62 | 2466.45 | 2215.14 | 1573.25 | 1129.79 |
| Gap set point(mm) | 22.27 | 17.27 | 10.5 | 9.27 | 7.27 | 4.5 | 4 |
| Roller speed (m/min) | 66.15 | 110.80 | 172.79 | 256.16 | 357.35 | 454.16 | 535.70 |

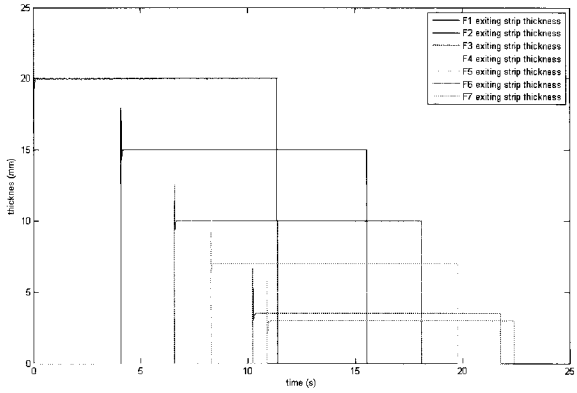


Fig. 8. Exiting strips' thickness of all finishing mills

Simulation condition was obtained by using the rolling process model based on practical parameters, it is assumed that an entry strip thickness disturbance whose amplitude is 5μm is initiated at the entry side of F1 stand and an entry force disturbance whose amplitude is 1000N is initiated at the entry side of F1 stand. The disturbance start at sample time 50s and end at sample time 51s while the total sample time is 80s.

(1) Strip entry thickness disturbance: an entry strip thickness disturbance whose amplitude is 5μm is initiated at the entry side of F1 stand, the thickness difference output of all the seven stands are listed below:

| No. stand | F1 | F2 | F3 | F4 | F5 | F6 | F7 |
|---|---|---|---|---|---|---|---|
| Thickness difference(μm) | 8.85 | 7.04 | 6.03 | 4.00 | 1.4 | 0.85 | 0.5 |

Force disturbance: an entry force disturbance whose amplitude is 1000N is initiated at the entry side of F1 stand, the thickness difference output of all the seven stands are listed below:

| No. stand | F1 | F2 | F3 | F4 | F5 | F6 | F7 |
|---|---|---|---|---|---|---|---|
| Thickness difference(μm) | 2.45 | 0.76 | 0.30 | 0.30 | 0.27 | 0.27 | 0.25 |

The results show that:

(1) The entry strip thickness changes and the force changes affect the strip thickness output of the rest stands. When the entry strip thickness changes reach 10μm, the strip exit thickness difference of the 1st stand the 7th stand reach 8.85μm and 0.5μm; when the entry roll force changes reach 1000N, the strip exit thickness difference of the 1st stand and 7th stand reach 2.45μm and 0.25μm ; The data in the list show that after adjustment by all the seven stands, the thickness difference of the last stand is less than 1μm. The exiting trip thickness difference is adjusted gradually by the seven stands reducing into the expected range.

(2) When the entry strip thickness disturbance type is adopted, the strip exit thickness difference reduces gradually until reached the expected range, when the entry strip roll force disturbance type is adopted, the strip exit thickness difference changes indistinctly except the 1st stand, because the 1st stand have eliminated the great mass of rolling influence.

## 4. Conclusions

In this paper, a gauge and strip tension control system for a hot strip finishing mill is presented. The simulation system can analyze most kinds of disturbance that affect the rolling process. The result of the simulation is quite close to the actual result. Intelligent control of a multi-function AGC system can greatly improve AGC control precision Module built in the paper can simulate the whole rolling process dynamically in order to get the best control effect. The design procedure can be extended to be used in the advanced control.

## References


[1] Nakagawa, S., Miura, H., Fukushima, S., and Armasaki, J, "Gauge control system for hot strip finishing mill," *Proc. 29th IEEE Conf. on Decision and Control*, Honolulu, HI, USA, 1990, pp. 1573–1578.

[2] Yoshiro Seki, Kunio Sekiguchi, "Optimal Multivariable Looper Control for Hot Strip Finishing Mill," *IEEE Transactions on industry applications*, vol.27, no.1, pp. 124-130, January/February 1991.

[3] M. Okada, Y. Iwasaki, "Optimal control system for hot strip finishing mill," *Proceedings of 35th, Conference on Decision and Control*, pp.1236-1241, Kobe, Japan, December 1996.

[4] Timothy Hesketh, "Controller Design for Hot Strip Finishing Mills," *IEEE transactions on control systems technology*, vol.6, no.2, pp. 208-219, March 1998.

[5] Lars M. Pedersen, "Multivariable thickness control of a hot rolling mill," *Tech. Rep., Lund Institute of technology*, September 1995.

[6] C.C. Roberts, "Mechanical principles of rolling," *Iron and Steel maker*, vol. 25, pp. 57-59, 1998.

[7] Konno Y. Development of hot rolling process simulator using GUI based simulation tool [A]. Steel Rolling 98 [C]. China, 1998.

[8] H. Imanari and Y. Morimatsu and K. Sekiguchi and H. Ezure and R. Matuoka and A. Tokuda and H. Otobe, "Looper H-Infinity control for hot strip mill," *IEEE Transactions on industry applications*, vol. 33, no. 3, pp. 790-796, 1997.

[9] T. Hesketh and D. J. Clements and D. H. Buttler and R. Lann, "Controller design for hot strip finishing mills," *IEEE Transactions on Control Systems Technology*, vol. 6, no. 2, pp. 208-219, 1998.

[10] K. Asano and K. Yamamoto and T. Kawase and N. Nomura, "Hot strip mill tension-looper control based on decentralization and coordination," *Control Engineering Practice*, vol. 8, no.3, pp. 337-344, 2000.

[11] H. Asada and A. Kitamura and S. Nishino and M. Konishi, "Adaptive and robust control method with estimation of rolling characteristics for looper angle control at hot strip mill," *ISLJ International*, vol. 43, no. 3, pp. 358-365, 2003.

[12] G. Hearns and P. Reeve and T.S. Bilkhu and P. Smith, "Multivariable guage and mass flow control for hot strip mills," *11th IFAC Symposium on Automation in Mining, Mineral and Metal Processing*, Nancy, France, 2004.

[13] F. Janabi-Sharifi, "A neuron-fuzzy system for looper tension control in rolling mills," *Control engineering practice*, vol. 13, no. 1, pp. 1-13, 2005.



**Xiaoying Wang**

He received his Bachelor in Nanjing University of Aeronautic and astronautic of China and master degrees in Shanghai Jiaotong University of China. His research interests are intelligent control and simulation etc.



**Jingcheng Wang**

He received his Bachelor and master degrees in Northwestern Polytechnic University of China and Ph.D. in Zhejiang University of China. He was a recipient of Alexander von Humboldt fellowship in Rostock University of Germany. Currently, he is a Professor in Shanghai Jiaotong University, Shanghai. His research interests are robust control, intelligent control, real-time control and simulation etc.